

Floquet-driven frictional effects

Vahid Mosallanejad ^{1,2,*}, Jingqi Chen ^{1,2} and Wenjie Dou^{1,2,3,†}

¹*Department of Chemistry, School of Science, Westlake University, Hangzhou, Zhejiang 310024, China*

²*Institute of Natural Sciences, Westlake Institute for Advanced Study, Hangzhou, Zhejiang 310024, China*

³*Department of Physics, School of Science, Westlake University, Hangzhou, Zhejiang 310024, China*



(Received 16 June 2022; revised 6 April 2023; accepted 16 May 2023; published 30 May 2023)

When the coupled electron-nuclear dynamics are subjected to strong Floquet driving, there is a strong breakdown of the Born-Oppenheimer approximation. In this paper, we derive a Fokker-Planck equation to describe nonadiabatic molecular dynamics with electronic friction for Floquet-driven systems. We first provide a new derivation of the Floquet quantum-classical Liouville equation (QCLE) for driven electron-nuclear dynamics. We then transform the Floquet QCLE into a Fokker-Planck equation with explicit forms of frictional force and random force. We recast the electronic friction in terms of Floquet Green's functions such that we can evaluate the electronic friction explicitly. We show that the Floquet electronic friction tensor exhibits antisymmetric terms even at the equilibrium for a real-valued Hamiltonian, suggesting that there is a Lorentz-like force in Floquet-driven non-Born Oppenheimer dynamics even without any spin-orbit couplings.

DOI: [10.1103/PhysRevB.107.184314](https://doi.org/10.1103/PhysRevB.107.184314)

I. INTRODUCTION

There are increasing interests in understanding of the dynamics of molecular systems exposed to strong light-matter interactions, which is helpful for interpreting photochemistry and spectroscopy [1,2]. For example, photoinduced molecular structure change in molecular junctions (MJs) is confirmed experimentally which highlights the importance of molecular dynamics in MJs [3,4]. In addition, theoretical solutions are given to reduce heating (improving structural stability) in MJs [5,6]. Light-driven phenomena is a broad ongoing research topic closely related to the larger topic Floquet-driven quantum systems which aims to understand the response of quantum systems to a periodic driving force often taking into account BO approximation [7–9]. In general, Floquet theorem provides a powerful method for the analysis of dynamical systems subjected to periodic external drivings. Effects, such as phase transitions and pump-probe photoemission can be explained by applying Floquet theorem in solving quantum mechanical problems [10–12]. However, Molecular dynamics near metallic surfaces can be nonadiabatic in nature and hence Born-Oppenheimer (BO) approximation is not necessary correct [13–15]. Recent studies begin to explore nonadiabatic contribution to the charge-current and thermodynamical properties of MJ [16]. In particular, people are interested in how to use light/photon to manipulate chemical and physical systems where the dynamical interplay between light and electronic nonadiabatic transitions plays a significant role [1]. Lacking appropriate treatments, our prime goal is to employ Floquet theorem for nonadiabatic molecular dynamics in presence of a periodic driving.

The electronic friction approach is considered as the first order correction to the BO approximation [17], which can be understood as a quantum mechanical damping force of a manifold of fast relaxing electronic on classical nuclear motion. Electronic friction approach is a practical way to carry out large-scale nonadiabatic molecular dynamics by replacing the electronic effects by the concept of electronic friction and were successful in explaining many experimental results such as molecular beam experiments [18–20], electrochemistry [21], charge/spin transport phenomena [22,23]. Quantitatively, electronic friction is a tensor which appears on the generalized Langevin equation [24]. One of the first notable quantum mechanical derivations of the electronic friction tensor is given by Head-Gordon and Tully [25]. Later, more rigorous expressions are derived from Keldysh Green's function [26,27], the path integral [28,29], the quantum classical Liouville equation (QCLE) [30], and the exact factorization [31]. It has been shown that there is only one universal electronic friction tensor in the Markovian limit [32,33]. Furthermore, studies shows that the friction tensor can exhibit antisymmetric terms in two situations: (1) out of equilibrium and (2) when spin-orbit couplings/complex-valued Hamiltonians are involved (even at equilibrium) [26,34]. The antisymmetric part of the friction tensor give a rise to an emergent Lorentz-like (Berry) force which in turn results in a closed trajectory (limit-cycle) for the nuclear degrees of freedom (DoFs) [26,35].

The coupled electron-nuclear dynamics with strong light-matter interactions can be described by the Floquet quantum classical Liouville equation (QCLE) successfully [36–38]. To confirm the correct Floquet QCLE, we offer a new derivation for the Floquet QCLE, starting from Floquet Liouville equation. Moreover, we map the Floquet QCLE into a Langevin equation with all nonadiabatic correction being incorporated into frictional effects. In the weak nonadiabatic

* vahid@westlake.edu.cn

† douwenjie@westlake.edu.cn

limit, the frictional terms are memoryless. Finally, to demonstrate usefulness of new derivations, we show that the Floquet electronic friction tensor exhibits antisymmetric terms even at the equilibrium for a real-valued Hamiltonian.

II. LIOUVILLE-VON NEUMANN EQUATION IN THE FLOQUET REPRESENTATION

For the coupled electron-nuclear motion, we consider a general Hamiltonian \hat{H} that is divided into the electronic Hamiltonian \hat{H}_e and the nuclear kinetic energy:

$$\hat{H} = \hat{H}^e(\mathbf{R}, t) + \sum_{\alpha} \frac{\hat{P}_{\alpha}^2}{2M_{\alpha}}. \quad (1)$$

Here $\mathbf{R} = \{R_{\alpha}\}$ and $\hat{\mathbf{P}} = \{\hat{P}_{\alpha}\}$ are the position and momentum operators for the nuclei, respectively. We use α to denote nuclear DoFs. Note that the electronic Hamiltonian $\hat{H}^e(\mathbf{R}, t)$ is considered to be an explicit function of \mathbf{R} and time t . Below, we will consider the case that the system is subjected to periodic driving, such that $\hat{H}^e(\mathbf{R}, t + T) = \hat{H}^e(\mathbf{R}, t)$ in which T is the period of the driving frequency.

The equation of motion for the coupled electron-nuclear density operator follows Liouville-von Neumann (LvN):

$$\frac{d\hat{\rho}(t)}{dt} = -\frac{i}{\hbar}[\hat{H}(t), \hat{\rho}(t)]. \quad (2)$$

For any periodic driving system, we can derive a Floquet Liouville-von Neumann (LvN) equation which describes the time evolution of the coupled density operator in the *Floquet representation*, as it will be denoted by $\rho_F(t)$. The motivation for such transformation stems from the fact the Floquet representation of a periodic Hamiltonian is time independent. Two major transformations are needed to derive Floquet representation of LvN: (I) transformation of LvN into the *Fourier representation* and (II) transformation from the Fourier representation to the Floquet representation.

The first transformation has two parts: (1) discrete expansion of the LvN in the Fourier space and (2) transferring from *Fourier expansion* to the Fourier representation. Part one begins by employing discrete Fourier expansions for both the time-dependent Hamiltonian and density operators as

$$\hat{H}(t) = \sum_n \hat{H}^{(n)} e^{in\omega t}, \quad \hat{\rho}(t) = \sum_n \hat{\rho}^{(n)}(t) e^{in\omega t}. \quad (3)$$

Note that coefficients $\hat{\rho}^{(n)}(t)$ are time-dependent whereas coefficients $\hat{H}^{(n)}$ are not. We then substitute above expansions on the LvN equation (4) as

$$\begin{aligned} & \sum_n \left(\frac{d\hat{\rho}^{(n)}(t)}{dt} e^{in\omega t} + in\omega \hat{\rho}^{(n)}(t) e^{in\omega t} \right) \\ &= -\frac{i}{\hbar} \sum_{k,m} [\hat{H}^{(k)}, \hat{\rho}^{(m)}(t)] e^{i(k+m)\omega t} \\ &= -\frac{i}{\hbar} \sum_{n,m} [\hat{H}^{(n-m)}, \hat{\rho}^{(m)}(t)] e^{in\omega t}. \end{aligned} \quad (4)$$

The step two of the first transformation begins by introducing the Floquet Number \hat{N} and the Floquet Ladder operators \hat{L}_n as

$$\hat{N}|n\rangle = n|n\rangle, \quad \hat{L}_n|m\rangle = |n+m\rangle. \quad (5)$$

In the matrix form, \hat{N} can be understood as a matrix with integer numbers on its diagonal and \hat{L}_n is an off-diagonal identity matrix shifted by n . Following relations are hold for these two operators:

$$\begin{aligned} [\hat{N}, \hat{L}_n] &= n\hat{L}_n, \quad [\hat{L}_n, \hat{L}_m] = 0, \\ \hat{L}_n \hat{L}_m &= \hat{L}_m \hat{L}_n = \hat{L}_{n+m}. \end{aligned} \quad (6)$$

Next, we introduce following Fourier representations as

$$\hat{H}^f(t) = \sum_n \hat{H}^{(n)} \hat{L}_n e^{in\omega t}, \quad \hat{\rho}^f(t) = \sum_n \hat{\rho}^{(n)}(t) \hat{L}_n e^{in\omega t}, \quad (7)$$

where we have modified Fourier expansions by adding the Ladder operator \hat{L}_n . We stress that, the Ladder operator turns the vector-like Fourier expansion into a matrixlike representation. Same way as Eq. (4), we substitute Fourier representations given above into Eq. (2) as

$$\begin{aligned} & \sum_n \left(\frac{d\hat{\rho}^{(n)}(t)}{dt} \hat{L}_n e^{in\omega t} + in\omega \hat{\rho}^{(n)}(t) \hat{L}_n e^{in\omega t} \right) \\ &= -\frac{i}{\hbar} \sum_{k,m} [\hat{H}^{(k)} \hat{L}_k, \hat{\rho}^{(m)} \hat{L}_m] e^{i(k+m)\omega t} \\ &= -\frac{i}{\hbar} \sum_{n,m} [\hat{H}^{(n-m)} \hat{L}_{n-m}, \hat{\rho}^{(m)} \hat{L}_m] e^{in\omega t} \\ &= -\frac{i}{\hbar} \sum_{n,m} [\hat{H}^{(n-m)}, \hat{\rho}^{(m)}] \hat{L}_n e^{in\omega t}, \end{aligned} \quad (8)$$

where we have used $[\hat{L}_{n-m}, \hat{L}_m] = 0$, and $\hat{L}_{n-m} \hat{L}_m = \hat{L}_n$ in the last line. Since for each n , two sides of Eqs. (4) and (8) are equivalent then we have proven that the LvN equation in Fourier representations keeps the original form as

$$\frac{d\hat{\rho}^f(t)}{dt} = -\frac{i}{\hbar} [\hat{H}^f(t), \hat{\rho}^f(t)]. \quad (9)$$

The transformation (II) begins by transforming the coupled density operator from its Fourier representation to the Floquet representation by

$$\hat{\rho}_F(t) = e^{-i\hat{N}\omega t} \hat{\rho}^f(t) e^{i\hat{N}\omega t} = \sum_n \hat{\rho}^{(n)}(t) \hat{L}_n. \quad (10)$$

By employing such a definition, the equation of motion for $\hat{\rho}_F(t)$ now reads as

$$\frac{d}{dt} \hat{\rho}_F(t) = -\frac{i}{\hbar} [\hat{H}_F, \hat{\rho}_F(t)], \quad (11)$$

where we have defined the following Floquet representation for the Hamiltonian as

$$\hat{H}_F = \sum_n \hat{H}^{(n)} \hat{L}_n + \hat{N} \hbar \omega. \quad (12)$$

We have used the commutation relations between the Ladder and Number operators, $[\hat{N}, \hat{L}_n] = n\hat{L}_n$, and $e^{-i\hat{N}\omega t} \hat{L}_n e^{i\hat{N}\omega t} = \hat{L}_n e^{-in\omega t}$ to derive the above equations. We emphasize that the Floquet LvN equation have the same structure as the traditional LvN. The advantage of the Floquet LvN is to allow us to program the dynamics using the time independent Hamiltonian. Equation (2) will be used as the starting point to derive the Floquet QCLE which further can be reduced to

the Fokker-Planck equation, i.e., the equation of motion for the nuclear DoFs. Notice that Eq. (11) is exact as long as the Hamiltonian is periodic.

III. FLOQUET QCLE

To derive the Floquet QCLE, we perform the partial Wigner transformation with respect to the nuclear DoFs on the Floquet LvN equation Eq. (11) as

$$\frac{d}{dt}(\hat{\rho}_F)_W(\mathbf{R}, \mathbf{P}, t) = -\frac{i}{\hbar}((\hat{H}_F \hat{\rho}_F)_W - (\hat{\rho}_F \hat{H}_F)_W). \quad (13)$$

We have used subscript W to denote the Wigner transformation. The Wigner transformation is given by

$$\hat{O}_W(\mathbf{R}, \mathbf{P}, t) \equiv \int d\mathbf{Y} e^{-\frac{i\mathbf{R}\cdot\mathbf{P}}{\hbar}} \left\langle \mathbf{R} - \frac{\mathbf{Y}}{2} \left| \hat{O}(t) \right| \mathbf{R} + \frac{\mathbf{Y}}{2} \right\rangle, \quad (14)$$

where $\hat{O}(t)$ is an arbitrary operator and $|\mathbf{R}\rangle$ is the real space representation of the nuclear DoFs. As a result of this transformation, \mathbf{R} and \mathbf{P} can be interpreted as position and momentum variables in the classical limit. Note that the Wigner-Moyal operator can be used to express the partial Wigner transform of the product of operators \hat{A} and \hat{B} :

$$\begin{aligned} (\hat{A}\hat{B})_W(\mathbf{R}, \mathbf{P}) &= \hat{A}_W(\mathbf{R}, \mathbf{P}) e^{-i\hbar \overleftrightarrow{\Lambda}/2} \hat{B}_W(\mathbf{R}, \mathbf{P}), \\ \overleftrightarrow{\Lambda} &= \sum_{\alpha} \frac{\overleftarrow{\partial}}{\partial P^{\alpha}} \frac{\overrightarrow{\partial}}{\partial R^{\alpha}} - \frac{\overleftarrow{\partial}}{\partial R^{\alpha}} \frac{\overrightarrow{\partial}}{\partial P^{\alpha}}. \end{aligned} \quad (15)$$

When truncating the Wigner-Moyal operator to the first order in the Taylor expansion, $e^{-i\hbar \overleftrightarrow{\Lambda}/2} \approx (1 - i\hbar \overleftrightarrow{\Lambda}/2)$, we arrive at the Floquet QCLE as

$$\begin{aligned} \frac{d}{dt} \hat{\rho}_{WF}(\mathbf{R}, \mathbf{P}, t) &= -i/\hbar [\hat{H}_{WF}, \hat{\rho}_{WF}(t)] \\ &\quad - \frac{1}{2} (\hat{H}_{WF} \overleftrightarrow{\Lambda} \hat{\rho}_{WF} - \hat{\rho}_{WF} \overleftrightarrow{\Lambda} \hat{H}_{WF}), \end{aligned} \quad (16)$$

Here, we have denoted $(\hat{O}_F)_W(\mathbf{R}, \mathbf{P}) \equiv \hat{O}_{WF}(\mathbf{R}, \mathbf{P})$. The subscript WF indicates that the Wigner transformation performed after the Floquet transformation. For the coupled electron-nuclear Hamiltonian in Eq. (1), we can rewrite the Floquet QCLE as follows:

$$\begin{aligned} \frac{\partial}{\partial t} \hat{\rho}_{WF}(t) &= -\hat{\mathcal{L}}_{WF}(\hat{\rho}_{WF}(t)) - \sum_{\alpha} \frac{P_{\alpha}}{M_{\alpha}} \frac{\partial \hat{\rho}_{WF}(t)}{\partial R_{\alpha}} \\ &\quad + \frac{1}{2} \sum_{\alpha} \left\{ \frac{\partial \hat{H}_{WF}^e}{\partial R_{\alpha}}, \frac{\partial \hat{\rho}_{WF}(t)}{\partial P_{\alpha}} \right\}. \end{aligned} \quad (17)$$

Here $\hat{\mathcal{L}}_{WF}(\hat{\rho}_{WF}(t)) \equiv i/\hbar [\hat{H}_{WF}^e, \hat{\rho}_{WF}(t)]$. \hat{H}_{WF}^e is the Floquet-Wigner transformed electronic Hamiltonian H^e . We have also denoted the anticommutator as $\{\hat{A}, \hat{B}\} = \hat{A}\hat{B} + \hat{B}\hat{A}$. Equation (17) is what we refer to as Floquet QCLE. Notice that in the literature, different ways of deriving Floquet QCLE are mentioned [39]. Such a Floquet QCLE represents the nonadiabatic dynamics of the coupled electron-nuclear motion subjected to periodic driving. Hereafter, we drop the index W for simplicity.

IV. DERIVATION OF FOKKER-PLANCK EQUATION

To arrive at an equation of motion just for the nuclear motion (Fokker-Planck equation), we denote the mixed nuclear-electron Floquet density operator $\hat{\rho}_F(\mathbf{R}, \mathbf{P}, t)$ as

$$\hat{\rho}_F(\mathbf{R}, \mathbf{P}, t) = \mathcal{A}(\mathbf{R}, \mathbf{P}, t) \hat{\rho}_F^{ss}(\mathbf{R}) + \hat{\mathcal{B}}(\mathbf{R}, \mathbf{P}, t). \quad (18)$$

Here the nuclear phase space density is denoted by $\mathcal{A}(\mathbf{R}, \mathbf{P}, t)$. The steady-state Floquet electronic density operator is denoted by $\hat{\rho}_F^{ss}(\mathbf{R})$. The difference operator, $\hat{\mathcal{B}}(\mathbf{R}, \mathbf{P}, t)$ is the density operator that counts for nonadiabatic effects. To be more explicit, we shall trace out the electronic and Floquet DoFs [30,40] as $\text{Tr}_{e,F}(\hat{\rho}_{WF}) = \mathcal{A}(\mathbf{R}, \mathbf{P}, t)$. Here, $\text{Tr}_{e,F}$ denotes trace over both many-body electronic states and Fourier space. Note that $\hat{\mathcal{L}}_F(\hat{\rho}_F^{ss}(\mathbf{R})) = 0$ and $\hat{\rho}_F^{ss}(\mathbf{R})$ is normalized on the electronic part at all \mathbf{R} such that $\text{Tr}_{e,F}(\hat{\rho}_F^{ss}(\mathbf{R})) = N$, where N is the Fourier space dimension. For further simplicity, we write a compact form of the Floquet QCLE, Eq. (16), as

$$\frac{d}{dt} \hat{\rho}_F(t) = -\hat{\mathcal{L}}_F(\hat{\rho}_F(t)) + \{\hat{H}_F^e, \hat{\rho}_F(t)\}_a, \quad (19)$$

where $\hat{\mathcal{L}}_F(\hat{\rho}_F(t)) \equiv i/\hbar [\hat{H}_F^e, \hat{\rho}_F(t)]$ and $\{\hat{A}, \hat{B}\}_a \equiv -1/2 (\hat{A} \overleftrightarrow{\Lambda} \hat{B} - \hat{B} \overleftrightarrow{\Lambda} \hat{A})$. We then substitute Eq. (18) in Eq. (19), and formally trace over the electronic bath and Fourier space as

$$\begin{aligned} \frac{\partial}{\partial t} \text{Tr}_{e,F}(\mathcal{A}(t) \hat{\rho}_F^{ss} + \hat{\mathcal{B}}) &= \text{Tr}_{e,F} \{ \hat{H}_F, \mathcal{A}(t) \hat{\rho}_F^{ss} \}_a \\ &\quad + \text{Tr}_{e,F} \{ \hat{H}_F, \hat{\mathcal{B}} \}_a. \end{aligned} \quad (20)$$

The detailed version of the above equation is given by

$$\begin{aligned} \frac{\partial}{\partial t} \mathcal{A}(t) &= - \sum_{\alpha} \left(\frac{P_{\alpha}}{M_{\alpha}} \right) \frac{\partial \mathcal{A}(t)}{\partial R_{\alpha}} + \frac{1}{2} \sum_{\alpha} \text{Tr}_{e,F} \\ &\quad \times \left(\frac{\partial \hat{H}_F^e}{\partial R_{\alpha}} \frac{\partial (\mathcal{A}(t) \hat{\rho}_F^{ss})}{\partial P_{\alpha}} + \frac{\partial (\mathcal{A}(t) \hat{\rho}_F^{ss})}{\partial P_{\alpha}} \frac{\partial \hat{H}_F^e}{\partial R_{\alpha}} \right) \\ &\quad + \frac{1}{2} \sum_{\alpha} \text{Tr}_{e,F} \left(\frac{\partial \hat{H}_F^e}{\partial R_{\alpha}} \frac{\partial \hat{\mathcal{B}}}{\partial P_{\alpha}} + \frac{\partial \hat{\mathcal{B}}}{\partial P_{\alpha}} \frac{\partial \hat{H}_F^e}{\partial R_{\alpha}} \right). \end{aligned} \quad (21)$$

Note that, $\text{Tr}_{e,F} \hat{\mathcal{L}}_F(\mathcal{A}(t) \hat{\rho}_F^{ss} + \hat{\mathcal{B}}) = \text{Tr}_{e,F} \hat{\mathcal{L}}_F(\hat{\mathcal{B}}) = 0$ and also $\text{Tr}_{e,F}(\partial \mathcal{B}/\partial R^{\alpha}) = 0$. The $\hat{\rho}_F^{ss}$ does not depend on P_{α} , and we can further simplify the above relation as

$$\begin{aligned} \frac{\partial}{\partial t} \mathcal{A}(t) &= - \sum_{\alpha} \left(\frac{P_{\alpha}}{M_{\alpha}} \right) \frac{\partial \mathcal{A}(t)}{\partial R_{\alpha}} + \sum_{\alpha} \text{Tr}_{e,F} \left(\frac{\partial \hat{H}_F^e}{\partial R_{\alpha}} \hat{\rho}_F^{ss} \right) \\ &\quad \times \frac{\partial \mathcal{A}(t)}{\partial P^{\alpha}} + \sum_{\alpha} \text{Tr}_{e,F} \left(\frac{\partial \hat{H}_F^e}{\partial R_{\alpha}} \frac{\partial \hat{\mathcal{B}}}{\partial P_{\alpha}} \right). \end{aligned} \quad (22)$$

To obtain the above relationship, we have used the fact that $\text{Tr}[AB] = \text{Tr}[BA]$. At this point, one needs to express $\hat{\mathcal{B}}$ in terms of $\hat{\mathcal{A}}$. To proceed, we can first have a relation for $\partial \hat{\mathcal{B}}/\partial t$ as

$$\begin{aligned} \frac{\partial}{\partial t} \hat{\mathcal{B}} &= -\hat{\rho}_F^{ss} \frac{\partial}{\partial t} \mathcal{A}(t) + \{ \hat{H}_F, \mathcal{A}(t) \hat{\rho}_F^{ss} \}_a + \{ \hat{H}_F, \hat{\mathcal{B}} \}_a \\ &\quad - \hat{\mathcal{L}}_F(\hat{\mathcal{B}}) = \{ \hat{H}_F, \hat{\mathcal{B}} \}_a - \hat{\rho}_F^{ss} \text{Tr}_{e,F} \{ \hat{H}_F, \hat{\mathcal{B}} \}_a \\ &\quad - \hat{\rho}_F^{ss} \text{Tr}_{e,F} \{ \hat{H}_F, \mathcal{A}(t) \hat{\rho}_F^{ss} \}_a \\ &\quad + \{ \hat{H}_F, \mathcal{A}(t) \hat{\rho}_F^{ss} \}_a - \hat{\mathcal{L}}_F(\hat{\mathcal{B}}). \end{aligned} \quad (23)$$

Next, we assume that nuclei move much slower than electrons. With that assumption, only the last three terms of the above relation will survive, such that we can have the following approximation for $\hat{\mathcal{B}}$:

$$\begin{aligned} \hat{\mathcal{L}}_F(\hat{\mathcal{B}}) &= -\hat{\rho}_F^{ss} \text{Tr}_{e,F} \{ \hat{H}_F, \mathcal{A}(t) \hat{\rho}_F^{ss} \}_a + \{ \hat{H}_F, \mathcal{A}(t) \hat{\rho}_F^{ss} \}_a \\ &= -\hat{\rho}_F^{ss} \left(-\sum_{\beta} \left(\frac{P_{\beta}}{M_{\beta}} \right) \frac{\partial \mathcal{A}(t)}{\partial R_{\beta}} \right. \\ &\quad + \sum_{\beta} \text{Tr}_{e,F} \left(\frac{\partial \hat{H}_F^e}{\partial R_{\beta}} \hat{\rho}_F^{ss} \right) \frac{\partial \mathcal{A}(t)}{\partial P_{\beta}} \Bigg) \\ &\quad - \sum_{\beta} \left(\frac{P_{\beta}}{M_{\beta}} \right) \left(\frac{\partial \mathcal{A}(t)}{\partial R_{\beta}} \hat{\rho}_F^{ss} + \frac{\partial \hat{\rho}_F^{ss}}{\partial R_{\beta}} \mathcal{A}(t) \right) \\ &\quad + \frac{1}{2} \sum_{\beta} \left(\frac{\partial \hat{H}_F^e}{\partial R_{\beta}} \hat{\rho}_F^{ss} + \hat{\rho}_F^{ss} \frac{\partial \hat{H}_F^e}{\partial R_{\beta}} \right) \frac{\partial \mathcal{A}(t)}{\partial P_{\beta}}. \end{aligned} \quad (24)$$

The above relation will be used to evaluate $\partial \hat{\mathcal{B}} / \partial P^{\alpha}$ as

$$\begin{aligned} \frac{\partial \hat{\mathcal{B}}}{\partial P_{\alpha}} &= -\sum_{\beta} \hat{\mathcal{L}}_F^{-1} \frac{\partial \hat{\rho}_F^{ss}}{\partial R_{\beta}} \frac{\partial}{\partial P_{\alpha}} \left(\left(\frac{P_{\beta}}{M_{\beta}} \right) \mathcal{A}(t) \right) \\ &\quad + \frac{1}{2} \sum_{\beta} \hat{\mathcal{L}}_F^{-1} \left(-\hat{\rho}_F^{ss} 2 \text{Tr}_{e,F} \left(\frac{\partial \hat{H}_F^e}{\partial R_{\beta}} \hat{\rho}_F^{ss} \right) \right. \\ &\quad \left. + \left(\frac{\partial \hat{H}_F^e}{\partial R_{\beta}} \hat{\rho}_F^{ss} + \hat{\rho}_F^{ss} \frac{\partial \hat{H}_F^e}{\partial R_{\beta}} \right) \right) \frac{\partial}{\partial P_{\alpha}} \frac{\partial \mathcal{A}(t)}{\partial P_{\beta}}. \end{aligned} \quad (25)$$

Then, the above expression will be substituted into Eq. (22), such that, to the first order in the correction to the BO approximation, we arrive at a Fokker-Planck equation for the pure nuclear density \mathcal{A} :

$$\begin{aligned} \frac{\partial}{\partial t} \mathcal{A} &= -\sum_{\alpha} \frac{P_{\alpha}}{m_{\alpha}} \frac{\partial \mathcal{A}}{\partial R_{\alpha}} - \sum_{\alpha} F_{\alpha} \frac{\partial \mathcal{A}}{\partial P_{\alpha}} \\ &\quad + \sum_{\alpha\beta} \gamma_{\alpha\beta} \frac{\partial}{\partial P_{\alpha}} \left(\frac{P_{\beta}}{m_{\beta}} \mathcal{A} \right) + \sum_{\alpha\beta} \bar{D}_{\alpha\beta} \frac{\partial^2 \mathcal{A}}{\partial P_{\alpha} \partial P_{\beta}}, \end{aligned} \quad (26)$$

in which, the mean force, F_{α} and friction tensor, $\gamma_{\alpha\beta}$, are

$$F_{\alpha} = \text{Tr}_{e,F} \left(\frac{\partial \hat{H}_F^e}{\partial R_{\alpha}} \hat{\rho}_F^{ss} \right), \quad (27)$$

$$\gamma_{\alpha\beta} = -\text{Tr}_{e,F} \left(\frac{\partial \hat{H}_F^e}{\partial R_{\alpha}} \hat{\mathcal{L}}_F^{-1} \frac{\partial \hat{\rho}_F^{ss}}{\partial R_{\beta}} \right). \quad (28)$$

The correlation function of the random force, $\bar{D}_{\alpha\beta}^S$, is also given by

$$\begin{aligned} \bar{D}_{\alpha\beta}^S &= \frac{1}{2} \text{Tr}_{e,F} \left(\frac{\partial \hat{H}_F^e}{\partial R_{\alpha}} \hat{\mathcal{L}}_F^{-1} \left(-\hat{\rho}_F^{ss} 2 \text{Tr}_{e,F} \left(\frac{\partial \hat{H}_F^e}{\partial R_{\beta}} \hat{\rho}_F^{ss} \right) \right. \right. \\ &\quad \left. \left. + \frac{\partial \hat{H}_F^e}{\partial R_{\beta}} \hat{\rho}_F^{ss} + \hat{\rho}_F^{ss} \frac{\partial \hat{H}_F^e}{\partial R_{\beta}} \right) \right). \end{aligned} \quad (29)$$

The Fokker-Planck equation is equivalent to the Langevin equation

$$m_{\alpha} \ddot{R}_{\alpha} = F_{\alpha} - \sum_{\beta} \gamma_{\alpha\beta} \dot{R}_{\beta} + \delta F_{\alpha}. \quad (30)$$

Here δF_{α} is the random force, which satisfies $\frac{1}{2} \langle \delta F_{\alpha}(0) \delta F_{\beta}(t) + \delta F_{\beta}(0) \delta F_{\alpha}(t) \rangle = \bar{D}_{\alpha\beta}^S \delta(t)$. $\gamma_{\alpha\beta}$ can be given as

$$\gamma_{\alpha\beta} = -\int_0^{\infty} dt \text{Tr}_{e,F} \left(\frac{\partial \hat{H}_F^e}{\partial R_{\alpha}} e^{-\frac{i\hat{H}_F^e t}{\hbar}} \frac{\partial \hat{\rho}_F^{ss}}{\partial R_{\beta}} e^{\frac{i\hat{H}_F^e t}{\hbar}} \right), \quad (31)$$

where we employed the identity $\hat{\mathcal{L}}_F^{-1}(\hat{O}) = \lim_{\eta \rightarrow 0^+} \int_0^{\infty} dt e^{-(\hat{\mathcal{L}}_F + \eta)t} \hat{O}$, in which $e^{-\hat{\mathcal{L}}_F t} \hat{O} = e^{-i\hat{H}_F^e t/\hbar} \hat{O} e^{i\hat{H}_F^e t/\hbar}$ (η being a positive infinitesimal). Up to now, we have successfully transformed the coupled electron-nuclear motion subjected to periodic driving into a Langevin equation for the pure nuclear motion with all electronic motion and Floquet driving being incorporated into frictional force and random force. From now on, we focus ourselves on the friction tensor and demonstrate that the friction can be expressed in terms of Green's functions. For a quadratic electronic Hamiltonian, $H^e = \sum_{ab} h_{ab}(\mathbf{R}, t) \hat{d}_a^{\dagger} \hat{d}_b + U(\mathbf{R})$, Eq. (31) can be expressed in terms of one-body electronic state as

$$\gamma_{\alpha\beta} = -\int_0^{\infty} dt \text{Tr}_{o,F} \left(\frac{\partial h_F}{\partial R_{\alpha}} e^{-\frac{i h_F t}{\hbar}} \frac{\partial \hat{\sigma}_F^{ss}}{\partial R_{\beta}} e^{\frac{i h_F t}{\hbar}} \right). \quad (32)$$

Here, $\text{Tr}_{o,F}$ denotes trace over both one-body electronic states, h_F represents the Floquet representation of the one-body Hamiltonian $h_{ab}(\mathbf{R}, t)$. Also, the matrix elements of the steady state one-body density operator defines as: $[\sigma_F^{ss}]_{ab} = \text{Tr}_e(\hat{d}_b^{\dagger} \hat{d}_a \hat{\rho}_F^{ss})$. Note that the potential for the nuclei, $U(R)$, does not contribute to the friction.

V. FRICTION IN TERMS OF ONE-BODY GREEN'S FUNCTION

One can recast the Floquet friction tensor into the energy domain as

$$\begin{aligned} \gamma_{\alpha\beta} &= -\int_0^{\infty} dt \int_0^{\infty} dt' \text{Tr}_{o,F} \left(\frac{\partial h_F}{\partial R_{\alpha}} e^{-\frac{i(h_F - i\eta)t}{\hbar}} \frac{\partial \sigma_F^{ss}}{\partial R_{\beta}} e^{\frac{i(h_F + i\eta)t'}{\hbar}} \right) \delta(t - t') \\ &= -\int_{-\infty}^{\infty} \frac{d\epsilon}{2\pi\hbar} \int_0^{\infty} dt \int_0^{\infty} dt' \text{Tr}_{o,F} \left(\frac{\partial h_F}{\partial R_{\alpha}} e^{-\frac{i(h_F - i\eta)t}{\hbar}} \frac{\partial \sigma_F^{ss}}{\partial R_{\beta}} e^{\frac{i(h_F + i\eta)t'}{\hbar}} \right) e^{i\epsilon(t-t')/\hbar} \\ &= -\hbar \int_{-\infty}^{\infty} \frac{d\epsilon}{2\pi} \text{Tr}_{o,F} \left(\frac{\partial h_F}{\partial R_{\alpha}} \frac{1}{\epsilon + i\eta - h_F} \frac{\partial \sigma_F^{ss}}{\partial R_{\beta}} \frac{1}{\epsilon - i\eta - h_F} \right). \end{aligned} \quad (33)$$

Hence, we have redefined the $\gamma_{\alpha\beta}$, partially, in terms of the Floquet retarded and advanced Green's functions, $G_F^{R/A} = (\epsilon \pm i\eta - h_F)^{-1}$, as

$$\gamma_{\alpha\beta} = -\hbar \int_{-\infty}^{\infty} \frac{d\epsilon}{2\pi} \text{Tr}_{o,F} \left(\frac{\partial h_F}{\partial R_\alpha} G_F^R \frac{\partial \sigma_F^{ss}}{\partial R_\beta} G_F^A \right). \quad (34)$$

The Floquet one-body density matrix can be further expressed in terms of Floquet lesser Green's function, such that the final expression for the Floquet electronic friction is given by

$$\gamma_{\alpha\beta} = \hbar \int_{-\infty}^{\infty} \frac{d\epsilon}{2\pi} \text{Tr}_{o,F} \left(\frac{\partial h_F}{\partial R_\alpha} \frac{\partial G_F^R}{\partial \epsilon} \frac{\partial h_F}{\partial R_\beta} G_F^< \right) + \text{H.c.}, \quad (35)$$

where $G_F^<$ is the lesser Floquet Green's function. See Appendix A for the details of derivation. Note that the Floquet electronic friction is the same as non-Floquet electronic friction, except Green's functions are now the Floquet version of the corresponding Green's function.

VI. DOT-LEAD SEPARATION

We now introduce a specific Hamiltonian model and Greens functions such that we can calculate the Floquet electronic friction explicitly. In the upcoming results section, we will demonstrate that the Floquet-driven electronic friction exhibits antisymmetric terms for a real Hamiltonian even when the dot is not biased (without any current). To be more specific, we consider a Hamiltonian with dot-lead separation:

$$\hat{H}_e = \hat{H}_s + \hat{H}_b + \hat{H}_v, \quad (36)$$

$$\hat{H}_s = \sum_{ij} [h^s]_{ij}(\mathbf{R}, t) \hat{d}_i^\dagger \hat{d}_j + U(\mathbf{R}), \quad (37)$$

$$\hat{H}_b = \sum_{\zeta k} \epsilon_{\zeta k} \hat{c}_{\zeta k}^\dagger \hat{c}_{\zeta k}, \quad (38)$$

$$\hat{H}_v = \sum_{\zeta k, i} V_{\zeta k, i} (\hat{c}_{\zeta k}^\dagger \hat{d}_i + \hat{d}_i^\dagger \hat{c}_{\zeta k}). \quad (39)$$

Here, \hat{H}_s is the dot Hamiltonian. The bath Hamiltonian consists of the left and right ($\zeta = L, R$) leads. \hat{H}_v describes the system-bath couplings. $U(\mathbf{R})$ is the potential for the nuclei.

For such a model, we can calculate Floquet Green's function exactly. In particular, the retarded Green's function for the system is given by

$$G_{sF}^R(\epsilon) = (\epsilon - \Sigma_F^R(\epsilon) - h_F^s)^{-1}, \quad (40)$$

$\Sigma_F^R(\epsilon) = \sum_{\zeta=L,R} \Sigma_{\zeta F}^R$ is the total self-energy in the Floquet representation. The elements of the self-energy is given by $[\Sigma_{\zeta F}^R]_{ij}(\epsilon) = \sum_k V_{\zeta k, i} g_{F, \zeta k}^R(\epsilon) V_{\zeta k, j}$, where the $g_{F, \zeta k}^R(\epsilon) = (\epsilon + i0^+ - \epsilon_{\zeta k} - \hat{N}\hbar\omega)^{-1}$ is the k th element of the retarded Green's function of the isolated lead ζ . h_F^s is the Floquet representation of the dot energy level. The lesser Green's function for the system is then given by

$$G_{sF}^<(\epsilon) = G_{sF}^R(\epsilon) \Sigma_F^<(\epsilon) G_{sF}^A(\epsilon), \quad (41)$$

Here, $\Sigma_F^<(\epsilon) = \sum_{\zeta=L,R} \Sigma_{\zeta F}^<(\epsilon)$ is the lesser Green's function, which can be evaluated as $[\Sigma_{\zeta F}^<]_{ij}(\epsilon) \equiv \sum_k V_{\zeta k, i} g_{F, \zeta k}^<(\epsilon) V_{\zeta k, j}$. Here, $g_{F, \zeta k}^<(\epsilon)$ is the lesser green's function for the ζ lead. $g_{F, \zeta k}^<(\epsilon) = i2\pi f(\epsilon - \hat{N}\hbar\omega - \mu_\zeta) \delta(\epsilon - \epsilon_{\zeta k} - \hat{N}\hbar\omega)$, where f is the Fermi function. In what following, we will invoke the

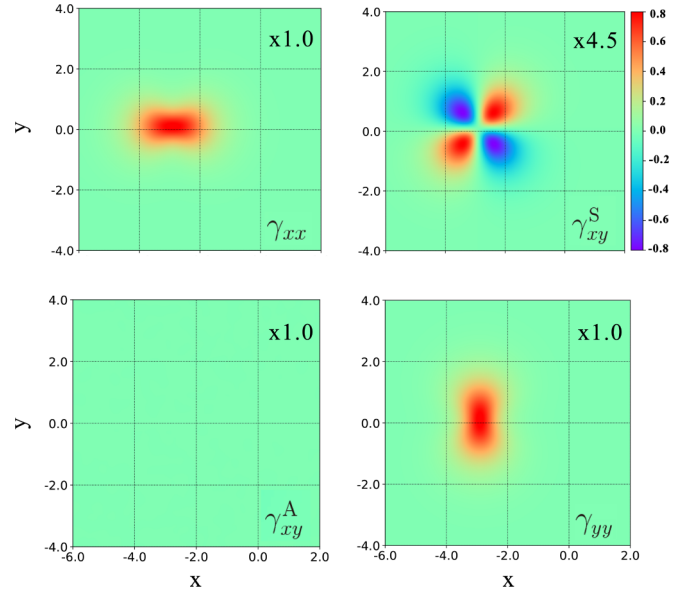


FIG. 1. Floquet friction tensors in absence of external driving $B = 0$: γ_{xx} (top left), γ_{xy}^S (top right), γ_{xy}^A (bottom left), and γ_{yy} (bottom right). Parameters: $\Gamma=1$, $\mu_{R,L} = 0$, $\beta = 2$, $A = 1$, $\Delta = 3$, and $\omega = 0.5$. We have used $N = 5$ Floquet levels to converge the results.

wide band approximation, such that $[\Sigma_{\zeta F}^R]_{ij}(\epsilon) = -\frac{i}{2}\Gamma_{ij}$, and $[\Sigma_{\zeta F}^<]_{ij}(\epsilon) = i\Gamma_{ij} f(\epsilon - \hat{N}\hbar\omega - \mu_\zeta)$. We can then proceed to calculate Floquet electronic friction using these Green's functions.

VII. RESULTS AND DISCUSSIONS

We will now consider a model consist of two-level orbital ($\pm\Delta$) coupled to two nuclear DoFs (x, y) and an off-diagonal periodic driving:

$$[h^s](x, y, t) = \begin{pmatrix} x + \Delta & Ay + B \cos(\omega t) \\ Ay + B \cos(\omega t) & -x - \Delta \end{pmatrix}. \quad (42)$$

The nuclear potential $U(\mathbf{R})$ is taken to be harmonic oscillators in both x and y dimensions. The diagonal terms of Hamiltonian represent two shifted parabolas in x direction with a driving force of 2Δ . The off-diagonal couplings depend on displacement in y direction as well as the term $B \cos(\omega t)$ which represents the interaction between an external monochromatic light source with the two shifted parabolas (the dipole approximation). B represents the strength of the external driving (e.g., the intensity of light) and ω is the frequency of the time-periodic driving. Below, we consider the case where the first level couples to the left lead and the second level couples to the right lead, and we set $\Gamma_{11} = \Gamma_{22} = \Gamma$.

In the equilibrium case (where $\mu_L = \mu_R$) and without any driving, the electronic friction is shown to be symmetric along nuclear DoFs provided the Hamiltonian is real [34]. In Fig. 1, we plot the friction tensors as a function of the nuclear coordinates (x, y). In particular, we define the symmetric and antisymmetric components $[\gamma_{xy}^S = (\gamma_{xy} + \gamma_{yx})/2, \gamma_{xy}^A = (\gamma_{xy} - \gamma_{yx})/2]$ of the friction tensor. In the absence of external driving ($B = 0$), the antisymmetric component is indeed vanished (as predicted). The frictions tensors γ_{xx} and γ_{yy} consists of two Gaussian curves which are merged along the

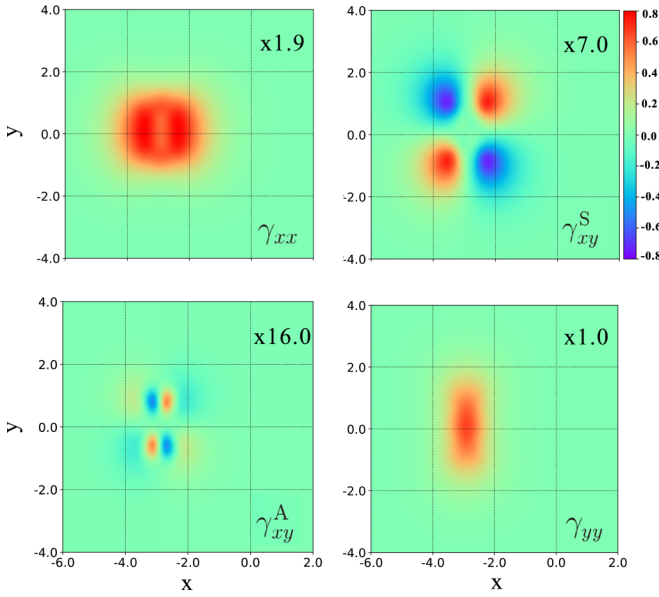


FIG. 2. Floquet friction tensors in presence of external driving: γ_{xx} (top left), γ_{xy}^S (top right), γ_{xy}^A (bottom left), and γ_{yy} (bottom right). Parameters: $\Gamma = 1$, $\mu_{R,L} = 0$, $\beta = 2$, $A = 1$, $\Delta = 3$, $\omega = 0.5$, $B = 1$, and $N = 5$.

orientations of the nuclear coordinate. This results agree with previous findings for real Hamiltonians without any driving [30,34].

We now turn on time-periodic off-diagonal coupling by setting $B = 1$. As shown in Fig. 2, the antisymmetric term γ_{xy}^A is no longer zero when Floquet driving is turning on. Moreover, the distributions of γ_{xx} , γ_{yy} , and γ_{xy}^S in the real space is enlarged as compared to the non-Floquet case. The magnitude of γ_{xx} and γ_{xy}^S are also increased by almost factor of 2. In general, electronic friction is large when two molecular energy surfaces meet each other (avoid-crossing points). In presence of the periodic driving, the single avoid-crossing between the two surface splits into multiple avoid-crossing between multiple quasi-energy surfaces. This can change the pattern of the friction tensors in a complicated way. For the Hamiltonian model of Eq. (42), the two closest quasi-surfaces have multiple avoid-crossing along the y direction. Consequently, the pattern of γ_{xx} broadened along the y -axis, whereas the γ_{yy} remains almost intact. For a comprehensive analysis of Floquet replicas see the quasi-energy surfaces in the Appendix B. Finally, in Fig. 3, we plot the frictional terms for the increased driving frequency ($\omega = 1$). In such a case, the magnitude of the antisymmetric terms (the Lorentz force) is notably increased, whereas the magnitudes of the other terms do not change significantly. Interestingly, the shape of γ_{xx} is composed of two large ellipses and two small ones. The central distance between the larger ellipse and the smaller one in x axis is about ω . This is consistent with the picture of Floquet replica of the potential surfaces separated by ω . Note that all friction terms have mirror symmetry around the avoided crossing point ($x = -\Delta$ and $y = 0$) and magnitudes of γ_{xy}^A and γ_{xy}^S are always maximized far from the avoided crossing. Finally, the pattern of γ_{xy}^A is different from that of spin-orbit couplings which was found to be Gaussian shape [34]. The

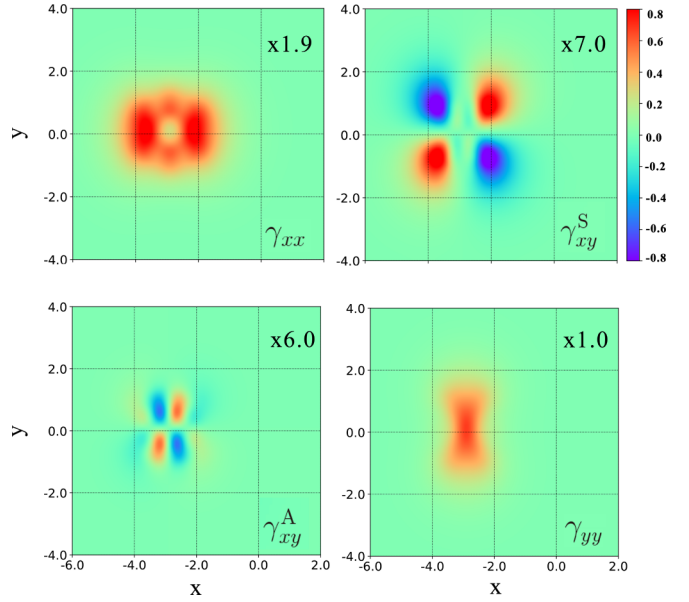


FIG. 3. Floquet Friction tensors in presence of external driving with a larger frequency: γ_{xx} (top left), γ_{xy}^S (top right), γ_{xy}^A (bottom left), and γ_{yy} (bottom right). Parameters: $\Gamma = 1$, $\mu_{R,L} = 0$, $\beta = 2$, $A = 1$, $\Delta = 3$, $\omega = 1$, $B = 1$, and $N = 5$.

magnitude of our γ_{xy}^A depends on the driven frequency and also is relatively smaller than that found for spin-orbit couplings.

VIII. CONCLUSION

We have formulated quantum-classical Liouville equation in Floquet representation to describe nonadiabatic dynamics with light-matter interactions. We have further mapped the Floquet QCLE into a Langevin dynamics where all electronic DoFs and light-matter interactions are incorporated into a friction tensor. We then recast the friction tensor into the form of Floquet Green's functions such that we can evaluate the friction tensor explicitly. We show that the light-matter interactions can introduce antisymmetric friction tensor even at equilibrium without any spin-orbit couplings. Future work must explore how the Lorentz-like force affects the dynamics in a realistic situation.

ACKNOWLEDGMENT

This material is based upon work supported by National Natural Science Foundation of China and (NSFC No. 22273075). V.M. acknowledge funding from Summer Academy Program for International Young Scientists (Grant No. GZWZ[2022]019). W.D. acknowledge the startup funding from Westlake University.

APPENDIX A: FURTHER SIMPLIFICATION OF THE FRICTION IN TERMS OF FLOQUET GREEN'S FUNCTION

For a practical calculation of electronic friction tensors, one needs to express the derivative $\partial\sigma_F^{ss}/\partial R_\beta$ in terms of the Floquet lesser Green's function denoted by $G_F^<$. The σ_F^{ss} relates to the $G_F^<$ by

$$\sigma_F^{ss} = \int \frac{d\epsilon'}{2\pi i} G_F^<(\epsilon') = \int \frac{d\epsilon'}{2\pi i} G_F^R(\epsilon') \Sigma_F^<(\epsilon') G_F^A(\epsilon'), \quad (\text{A1})$$

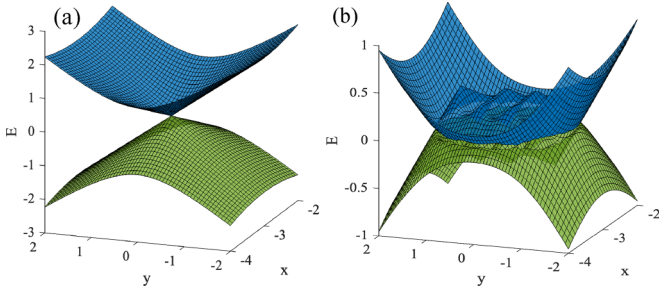


FIG. 4. (a) The single avoid crossing (no light). (b) closest quasi surfaces for $\omega = 0.5$.

where $\Sigma_F^<$ is the total lead's Floquet lesser self-energy [41]. Here, we have adopted a dot-lead (system-bath) separation. Furthermore, we have assumed that $\Sigma_F^<$ neither depends on the energy ϵ' (so-called wide-band approximation) nor on the position \mathbf{R} (so-called Condon approximation). Note that the wide-band approximation allows us to express the lesser green's function in the Floquet representation as $G_F^<(\epsilon') = G_F^R(\epsilon')\Sigma_F^<G_F^A(\epsilon')$. In addition with Condon approximation, one can easily derive the following identity:

$$\frac{\partial G_F^<}{\partial R_\beta} = G_F^R \frac{\partial h_F}{\partial R_\beta} G_F^< + G_F^< \frac{\partial h_F}{\partial R_\beta} G_F^A. \quad (\text{A2})$$

Note that it is not practical to directly evaluate $\partial \sigma_F^{ss} / \partial R_\beta$ from Eq. (A1) and substitute it into Eq. (34) due to extra integration over ϵ' . To proceed further, we can replace the $\text{Tr}_{\alpha,F}(\dots)$ with $\sum_n \langle n | \dots | n \rangle$ in the last line of Eq. (34) and use the eigenbasis of the Floquet electronic Hamiltonian, $h_F |n\rangle = \epsilon_n |n\rangle$, as

$$\begin{aligned} \gamma_{\alpha\beta} &= -\hbar \sum_n \int_{-\infty}^{\infty} \frac{d\epsilon}{2\pi} \langle n | \frac{\partial h_F}{\partial R_\alpha} \frac{1}{\epsilon + i\eta - h_F} \frac{\partial \sigma_F^{ss}}{\partial R_\beta} | n \rangle \\ &\quad \times \frac{1}{\epsilon - i\eta - \epsilon_n}. \end{aligned} \quad (\text{A3})$$

Next, we will use the Floquet identity operator $\sum_m |m\rangle \langle m|$ as

$$\begin{aligned} \gamma_{\alpha\beta} &= -\hbar \sum_{n,m} \int_{-\infty}^{\infty} \frac{d\epsilon}{2\pi} \langle n | \frac{\partial h_F}{\partial R_\alpha} | m \rangle \frac{1}{\epsilon + i\eta - \epsilon_m} \\ &\quad \times \langle m | \frac{\partial \sigma_F^{ss}}{\partial R_\beta} | n \rangle \frac{1}{\epsilon - i\eta - \epsilon_n}. \end{aligned} \quad (\text{A4})$$

Next, we will use the Floquet identity operator $\sum_m |m\rangle \langle m|$ as

$$\begin{aligned} \gamma_{\alpha\beta} &= -\hbar \sum_{n,m} \int_{-\infty}^{\infty} \frac{d\epsilon}{2\pi} \langle n | \frac{\partial h_F}{\partial R_\alpha} | m \rangle \frac{1}{\epsilon + i\eta - \epsilon_m} \\ &\quad \times \langle m | \frac{\partial \sigma_F^{ss}}{\partial R_\beta} | n \rangle \frac{1}{\epsilon - i\eta - \epsilon_n}. \end{aligned} \quad (\text{A5})$$

Taking the singularity point at $\epsilon = i\eta + \epsilon_n$ and using the residue theorem for contour integration leads to

$$\begin{aligned} \gamma_{\alpha\beta} &= -i\hbar \sum_{n,m} \langle n | \frac{\partial h_F}{\partial R_\alpha} | m \rangle \frac{1}{\epsilon_n - \epsilon_m + i2\eta} \\ &\quad \times \langle m | \frac{\partial \sigma_F^{ss}}{\partial R_\beta} | n \rangle. \end{aligned} \quad (\text{A6})$$

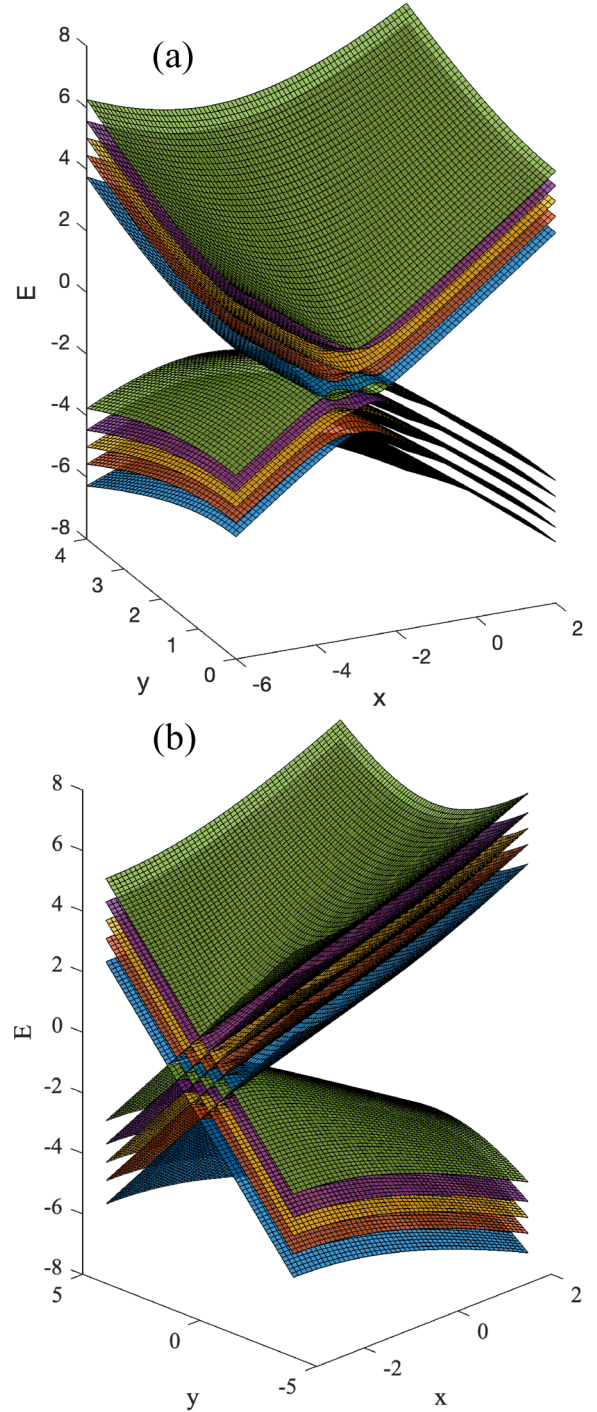


FIG. 5. (a) The cross-section of Floquet replicas for $\omega = 0.5$ along the x axis (associated with Fig. 2). (b) Same as (a) along the y axis.

At this point, we will evaluate the last term of above expression as: $\langle m | \frac{\partial \sigma_F^{ss}}{\partial R_\beta} | n \rangle$. According to Eqs. (A1) and (A2), this term has two parts as

$$\begin{aligned} \langle m | \frac{\partial \sigma_F^{ss}}{\partial R_\beta} | n \rangle &= \int \frac{d\epsilon'}{2\pi i} \langle m | G_F^R(\epsilon') \frac{\partial h_F}{\partial R_\beta} G_F^R(\epsilon') \Sigma_F^< G_F^A(\epsilon') | n \rangle \\ &\quad + \langle m | G_F^R(\epsilon') \Sigma_F^< G_F^A(\epsilon') \frac{\partial h_F}{\partial R_\beta} G_F^A(\epsilon') | n \rangle. \end{aligned} \quad (\text{A7})$$

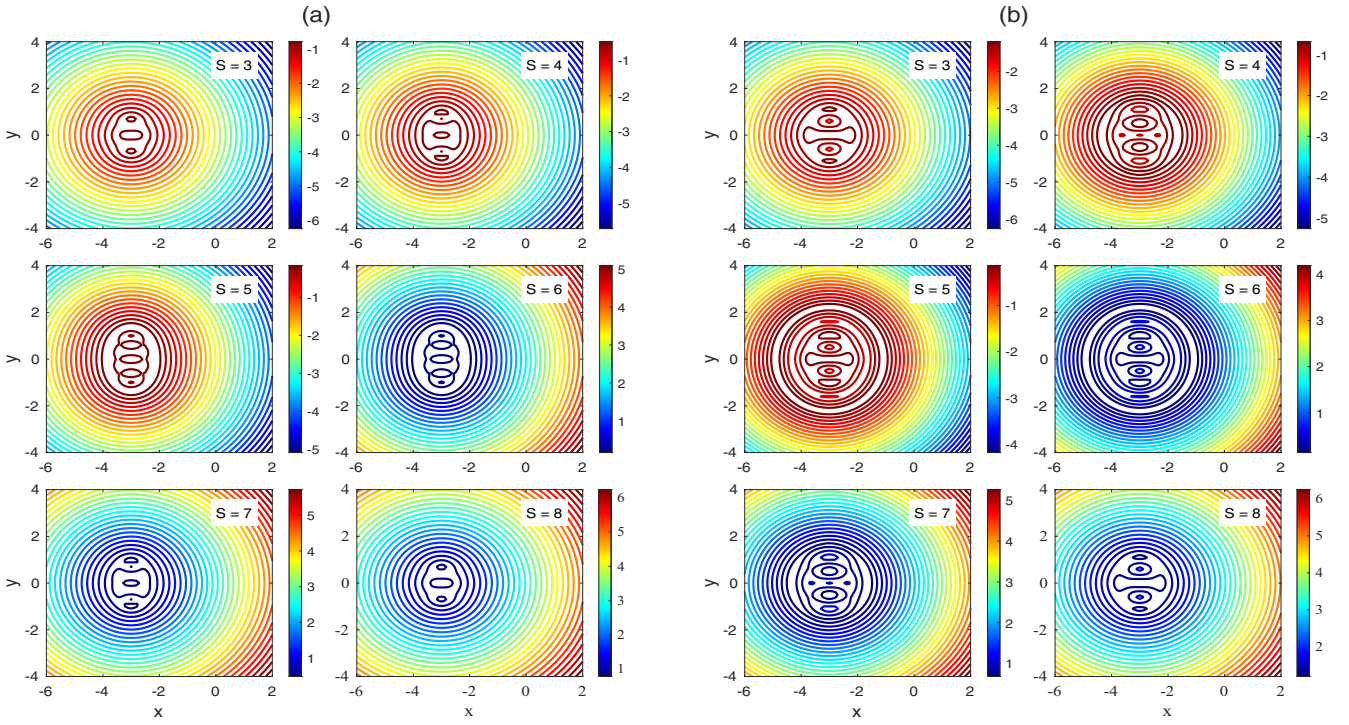


FIG. 6. (a) Contour plots of Floquet replicas for $\omega = 0.5$. (b) same as (a) for $\omega = 1$.

The integration over ϵ' can be accomplished by using the eigenbasis of the Floquet electronic Hamiltonian and employing the identity operator $\sum_{m'} |m'\rangle\langle m'|$. The first part is given by

$$\begin{aligned} & \sum_{m'} \int \frac{d\epsilon'}{2\pi i} \frac{1}{\epsilon' + i\eta - \epsilon_m} \langle m | \frac{\partial h_F}{\partial R_\beta} | m' \rangle \frac{1}{\epsilon' + i\eta - \epsilon_{m'}} \\ & \quad \times \langle m' | \Sigma_F^< | n \rangle \frac{1}{\epsilon' - i\eta - \epsilon_n} \\ & = \sum_{m'} \frac{1}{\epsilon_n - \epsilon_m + i2\eta} \\ & \quad \times \langle m | \frac{\partial h_F}{\partial R_\beta} | m' \rangle \frac{1}{\epsilon_n - \epsilon_{m'} + i2\eta} \langle m' | \Sigma_F^< | n \rangle. \quad (\text{A8}) \end{aligned}$$

Similarly (by taking the singularity point at $\epsilon' = -i\eta + \epsilon_{m'}$), the second part reduces to

$$\begin{aligned} & \sum_{m'} \langle m | \Sigma_F^< | m' \rangle \frac{1}{\epsilon_m - \epsilon_{m'} - i2\eta} \langle m' | \frac{\partial h_F}{\partial R_\beta} | n \rangle \\ & \quad \times \frac{1}{\epsilon_m - \epsilon_n - i2\eta}. \quad (\text{A9}) \end{aligned}$$

A relation for $\gamma_{\alpha\beta}$ can be derived by substitution of these two parts in the Eq. (A5) as

$$\begin{aligned} \gamma_{\alpha\beta} & = -i\hbar \sum_{n,m,m'} \langle n | \frac{\partial h_F}{\partial R_\alpha} | m \rangle \frac{1}{\epsilon_n - \epsilon_m + i2\eta} \\ & \quad \times \left(\frac{1}{\epsilon_n - \epsilon_m + i2\eta} \langle m | \frac{\partial h_F}{\partial R_\beta} | m' \rangle \frac{1}{\epsilon_n - \epsilon_{m'} + i2\eta} \right. \\ & \quad \times \langle m' | \Sigma_F^< | n \rangle + \langle m | \Sigma_F^< | m' \rangle \frac{1}{\epsilon_m - \epsilon_{m'} - i2\eta} \langle m' | \frac{\partial h_F}{\partial R_\beta} | n \rangle \\ & \quad \left. \times \frac{1}{\epsilon_m - \epsilon_n - i2\eta} \right). \quad (\text{A10}) \end{aligned}$$

Taking similar procedures [replacing $\text{Tr}_{o,F}(\dots)$ by $\sum_n \langle n | \dots | n \rangle$, using the eigenbasis of the Floquet electronic Hamiltonian and employing the identity operators], one can conclude that the following general single integration formula

$$\begin{aligned} \gamma_{\alpha\beta} & = \hbar \int_{-\infty}^{\infty} \frac{d\epsilon}{2\pi} \text{Tr}_{o,F} \left(\frac{\partial h_F}{\partial R_\alpha} \frac{\partial G_F^R}{\partial \epsilon} \frac{\partial h_F}{\partial R_\beta} G_F^< \right. \\ & \quad \left. - \frac{\partial h_F}{\partial R_\alpha} G_F^< \frac{\partial h_F}{\partial R_\beta} \frac{\partial G_F^A}{\partial \epsilon} \right), \quad (\text{A11}) \end{aligned}$$

delivers a similar outputs as Eq. (A10). Note that, we have used the identity $\partial G_F^{R,A} / \partial \epsilon = -G_F^{R,A} G_F^{R,A}$ [40]. This relation is a practical formula for evaluation of $\gamma_{\alpha\beta}$. The second term in Eq. (A10) is also the hermitian conjugate of the first part. Since the trace in any basis set is the same, Eq. (A11) represents a general form for Floquet electronic friction.

APPENDIX B: FLOQUET REPLICAS

In order to better justify the pattern of electronic frictions plotted in Figs. 2 and 3, we first plot the single avoided crossing point in the absence of light [based on Eq. (42)] in Fig. 4(a) and then we plot the two closest quasienergy surfaces for $\omega = 0.5$ [based on $h_F^s(x, y)$] in Fig. 4(b). In particular, single avoided crossing point splits into complex multiple avoid-crossing points. For the two-level system with $N = 5$, there are 10 replicas which we will identify each with S . Indeed, the two closest surfaces are $S = 5$ and 6. We also plot two cross sections of all Floquet replicas corresponding to Fig. 2 in Figs. 5(a) and 5(b). In addition, we plotted contour plots of few quasi-surfaces that are corresponds to Figs. 2 and 3 in Figs. 6(a) and 6(b), respectively. One can see the pattern of contour plots for $S = 5$ and 6 are more complicated when $\omega = 1$ and special distribution of γ_{xx} roughly follows the two

iso-surfaces of $S = 5$ and 6. Another important point is that, quasi avoided crossing points are introduced symmetrically

around the axis $y = 0$ and that is the reason the γ_{yy} does not altered as much as γ_{xx} .

-
- [1] M. Schirò, F. G. Eich, and F. Agostini, Quantum–classical nonadiabatic dynamics of floquet driven systems, *J. Chem. Phys.* **154**, 114101 (2021).
- [2] J. E. Lang, R.-B. Liu, and T. S. Monteiro, Dynamical-Decoupling-Based Quantum Sensing: Floquet Spectroscopy, *Phys. Rev. X* **5**, 041016 (2015).
- [3] H. Liu, Y. Xu, F. Li, Y. Yang, W. Wang, Y. Song, and D. Liu, Light-driven conformational switch of i-motif dna, *Angew. Chem., Int. Ed.* **46**, 2515 (2007).
- [4] Z. Bei, Y. Huang, Y. Chen, Y. Cao, and J. Li, Photo-induced carbocation-enhanced charge transport in single-molecule junctions, *Chem. Sci.* **11**, 6026 (2020).
- [5] M. Kuperman, L. Nagar, and U. Peskin, Mechanical stabilization of nanoscale conductors by plasmon oscillations, *Nano Lett.* **20**, 5531 (2020).
- [6] R. J. Preston, T. D. Honeychurch, and D. S. Kosov, Cooling molecular electronic junctions by ac current, *J. Chem. Phys.* **153**, 121102 (2020).
- [7] H. Sambe, Steady states and quasienergies of a quantum-mechanical system in an oscillating field, *Phys. Rev. A* **7**, 2203 (1973).
- [8] S. Kohler, J. Lehmann, and P. Hänggi, Driven quantum transport on the nanoscale, *Phys. Rep.* **406**, 379 (2005).
- [9] V. Novičenko, E. Anisimovas, and G. Juzeliūnas, Floquet analysis of a quantum system with modulated periodic driving, *Phys. Rev. A* **95**, 023615 (2017).
- [10] K. Yang, L. Zhou, W. Ma, X. Kong, P. Wang, X. Qin, X. Rong, Y. Wang, F. Shi, J. Gong *et al.*, Floquet dynamical quantum phase transitions, *Phys. Rev. B* **100**, 085308 (2019).
- [11] H. Dehghani, T. Oka, and A. Mitra, Dissipative floquet topological systems, *Phys. Rev. B* **90**, 195429 (2014).
- [12] M. Sentef, M. Claassen, A. Kemper, B. Moritz, T. Oka, J. Freericks, and T. Devereaux, Theory of floquet band formation and local pseudospin textures in pump-probe photoemission of graphene, *Nat. Commun.* **6**, 7047 (2015).
- [13] S. P. Rittmeyer, V. J. Bukas, and K. Reuter, Energy dissipation at metal surfaces, *Adv. Phys.: X* **3**, 1381574 (2018).
- [14] M. Galperin and A. Nitzan, Nuclear dynamics at molecule–metal interfaces: A pseudoparticle perspective, *J. Phys. Chem. Lett.* **6**, 4898 (2015).
- [15] J. I. Juaristi, M. Alducin, R. D. Muiño, H. F. Busnengo, and A. Salin, Role of Electron-Hole Pair Excitations in the Dissociative Adsorption of Diatomic Molecules on Metal Surfaces, *Phys. Rev. Lett.* **100**, 116102 (2008).
- [16] J. Bätge, A. Levy, W. Dou, and M. Thoss, Nonadiabatically driven open quantum systems under out-of-equilibrium conditions: Effect of electron-phonon interaction, *Phys. Rev. B* **106**, 075419 (2022).
- [17] W. Dou and J. E. Subotnik, Perspective: How to understand electronic friction, *J. Chem. Phys.* **148**, 230901 (2018).
- [18] P. Spiering and J. Meyer, Testing electronic friction models: vibrational de-excitation in scattering of H₂ and D₂ from Cu(111), *J. Phys. Chem. Lett.* **9**, 1803 (2018).
- [19] J.-T. Lü, B.-Z. Hu, P. Hedegård, and M. Brandbyge, Semi-classical generalized langevin equation for equilibrium and nonequilibrium molecular dynamics simulation, *Prog. Surf. Sci.* **94**, 21 (2019).
- [20] N. Hertl, R. Martin-Barrios, O. Galparsoro, P. Larrégaray, D. J. Auerbach, D. Schwarzer, A. M. Wodtke, and A. Kandratsenka, Random force in molecular dynamics with electronic friction, *J. Phys. Chem. C* **125**, 14468 (2021).
- [21] Y.-C. Lam, A. V. Soudackov, Z. K. Goldsmith, and S. Hammes-Schiffer, Theory of proton discharge on metal electrodes: electronically adiabatic model, *J. Phys. Chem. C* **123**, 12335 (2019).
- [22] W. Dou, C. Schinabeck, M. Thoss, and J. E. Subotnik, A broadened classical master equation approach for treating electron-nuclear coupling in non-equilibrium transport, *J. Chem. Phys.* **148**, 102317 (2018).
- [23] U. Bajpai and B. K. Nikolić, Spintronics Meets Nonadiabatic Molecular Dynamics: Geometric Spin Torque and Damping on Dynamical Classical Magnetic Texture due to an Electronic Open Quantum System, *Phys. Rev. Lett.* **125**, 187202 (2020).
- [24] M. Askerka, R. J. Maurer, V. S. Batista, and J. C. Tully, Role of Tensorial Electronic Friction in Energy Transfer at Metal Surfaces, *Phys. Rev. Lett.* **116**, 217601 (2016).
- [25] M. Head-Gordon and J. C. Tully, Molecular dynamics with electronic frictions, *J. Chem. Phys.* **103**, 10137 (1995).
- [26] N. Bode, S. V. Kusminskiy, R. Egger, and F. von Oppen, Current-induced forces in mesoscopic systems: A scattering-matrix approach, *Beilstein J. Nanotechnol.* **3**, 144 (2012).
- [27] V. F. Kershaw and D. S. Kosov, Non-adiabatic effects of nuclear motion in quantum transport of electrons: A self-consistent keldysh–langevin study, *J. Chem. Phys.* **153**, 154101 (2020).
- [28] J.-T. Lü, M. Brandbyge, P. Hedegård, T. N. Todorov, and D. Dundas, Current-induced atomic dynamics, instabilities, and raman signals: Quasiclassical langevin equation approach, *Phys. Rev. B* **85**, 245444 (2012).
- [29] F. Chen, K. Miwa, and M. Galperin, Electronic friction in interacting systems, *J. Chem. Phys.* **150**, 174101 (2019).
- [30] W. Dou and J. E. Subotnik, A many-body states picture of electronic friction: The case of multiple orbitals and multiple electronic states, *J. Chem. Phys.* **145**, 054102 (2016).
- [31] R. Martinazzo and I. Burghardt, Quantum Dynamics with Electronic Friction, *Phys. Rev. Lett.* **128**, 206002 (2022).
- [32] W. Dou and J. E. Subotnik, Universality of electronic friction: Equivalence of von Oppen’s nonequilibrium Green’s function approach and the Head-Gordon–Tully model at equilibrium, *Phys. Rev. B* **96**, 104305 (2017).
- [33] W. Dou and J. E. Subotnik, Universality of electronic friction. II. Equivalence of the quantum-classical Liouville equation approach with von Oppen’s nonequilibrium Green’s function methods out of equilibrium, *Phys. Rev. B* **97**, 064303 (2018).
- [34] H.-H. Teh, W. Dou, and J. E. Subotnik, Antisymmetric berry frictional force at equilibrium in the presence of spin-orbit coupling, *Phys. Rev. B* **104**, L201409 (2021).

- [35] H.-H. Teh, W. Dou, and J. E. Subotnik, Spin polarization through a molecular junction based on nuclear berry curvature effects, *Phys. Rev. B* **106**, 184302 (2022).
- [36] R. Kapral, Progress in the theory of mixed quantum-classical dynamics, *Annu. Rev. Phys. Chem.* **57**, 129 (2006).
- [37] A. Kelly and R. Kapral, Quantum-classical description of environmental effects on electronic dynamics at conical intersections, *J. Chem. Phys.* **133**, 084502 (2010).
- [38] H. Kim, A. Nassimi, and R. Kapral, Quantum-classical liouville dynamics in the mapping basis, *J. Chem. Phys.* **129**, 084102 (2008).
- [39] H.-T. Chen, Z. Zhou, and J. E. Subotnik, On the proper derivation of the floquet-based quantum classical liouville equation and surface hopping describing a molecule or material subject to an external field, *J. Chem. Phys.* **153**, 044116 (2020).
- [40] W. Dou, G. Miao, and J. E. Subotnik, Born-Oppenheimer Dynamics, Electronic Friction, and the Inclusion of Electron-Electron Interactions, *Phys. Rev. Lett.* **119**, 046001 (2017).
- [41] H. H. Yap, L. Zhou, J.-S. Wang, and J. Gong, Computational study of the two-terminal transport of Floquet quantum Hall insulators, *Phys. Rev. B* **96**, 165443 (2017).